

To what extent can the Λ CDM Model explain the Missing Satellite Problem?

Madhav Menon

October 7, 2022

Abstract

Disparities between N-body simulations and real-life observations have shown that there should exist more satellites than observed. Using CLASS, a total of five dark matter particles were modelled. Their consequent Matter Power Spectrums and Relative Transfer Functions to Λ CDM were plotted in order to understand their breaking points which help extrapolate the relative magnitudes of their free streaming length qualitatively. It was found that warmer dark matter models have greater free-streaming length which helps maintain smaller scale structures and shows that the number of satellites that would be formed in a warm dark matter model universe would roughly correspond to the results devised by N-body simulations.

Contents

1	Introduction	3
1.1	The context for dark matter	3
1.2	The Λ CDM model	6
1.3	The Missing Sattelite Problem	7
1.4	MPKs	7
1.5	Transfer functions	9
2	Analysis of Dark Matter Models	10
2.1	Λ CDM	10
2.2	WDM Neutrino	11
2.3	Changing g_x and fitting $T(k)$	13
	Conclusion	15
	Acknowledgements	16
	References	16

1 Introduction

1.1 The context for dark matter

While dark matter is a phrase that is thrown around when it comes to popular science, it serves as a useful model to help explain various cosmological phenomena that have been observed over the past decades. In order to understand one of the main reasons for the discovery of dark matter, we begin by analysing the orbital velocity of the planets in our solar system. By assuming a perfect circular orbit, we get that the gravitational force between the planet and the sun is given by

$$F_g = G \frac{M_{planet} M_{\odot}}{R^2} \quad (1)$$

where M_{\odot} is the mass of the sun and r is the distance between the centre of mass of the sun and a planet. Similarly, the centripetal force of the planet is given by

$$F_c = \frac{M_{planet} v^2}{R} \quad (2)$$

By equating (1) and (2), we can solve for the orbital velocity as a function of r to give us

$$v = \sqrt{G \frac{M_{\odot}}{R}} \quad (3)$$

This allows us to establish the relationship

$$v \propto \frac{1}{\sqrt{R}} \quad (4)$$

Plotting v against R for planets against our solar system gives us a rotation curve as shown in figure 1.

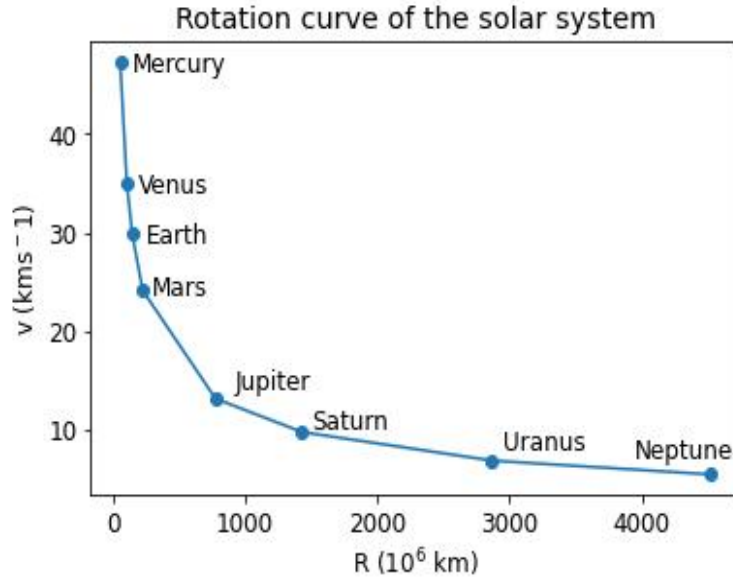


Figure 1: Rotation Curve of the Solar System (Williams, 2010)

In the 1930s, Swiss astronomer Fritz Zwicky, revolutionised the world of Modern Astrophysics. After studying data from the Coma Cluster, a large galaxy cluster about 99 Mpc away from earth, Zwicky discovered that the apparent velocities of the 8 galaxies within this cluster was too high for its mass. He came up with the idea of dark matter in order to explain it.

Later, Vera Rubin had the idea of extrapolating this to galaxies. After gathering data on over 60 galaxies, it was found out that as $R \rightarrow 30 \text{ kpc}$, the rotation curves start to flatten out as shown in Figure 2. This discovery was significant as it proved that the orbital velocity of stellar structures towards the edge of M31 is approximately the orbital velocity of those near the core of the galaxy. This is significantly different from the rotation curve of the solar system, thus showing that there needs to be additional mass in the galaxy to maintain its structural integrity. Dark matter is invoked as a substance that provides this mass.

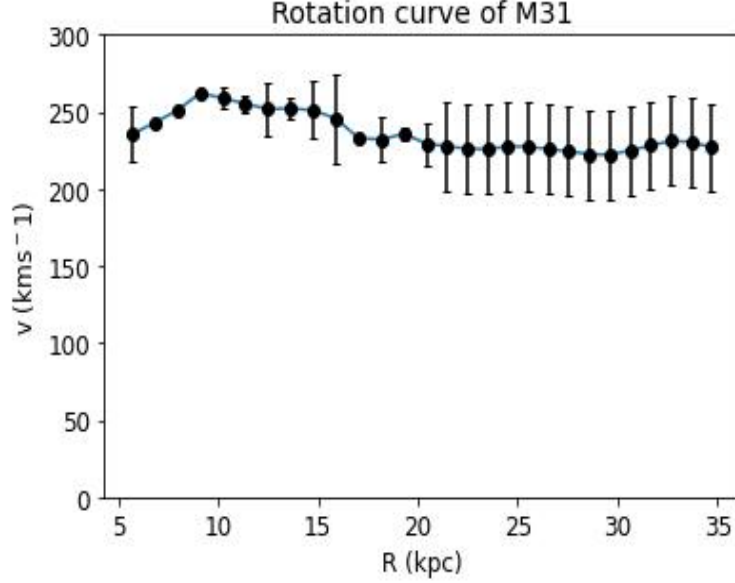


Figure 2: Rotation Curve of M31
(Carignan et al., 2006)

In fact, we can even determine the percentage of our universe that is composed of dark matter. By probing the critical density $\rho_c \approx 10^{-26} \text{kgm}^{-3}$ (Dodelson & Schmidt, 2020), we can express the density parameter of essentially any substance in our universe as

$$\Omega_{parameter} = \frac{\rho_{parameter}}{\rho_c} \quad (5)$$

Through various astrophysical methods, cosmologists have been able to determine that the density parameter of baryons $\Omega_B \approx 0.05$ (Dodelson & Schmidt, 2020). This allows us to extrapolate that the density parameter of dark matter $\Omega_{dm} \approx 0.3$, which tells us that about 30% of our universe is comprised of dark matter (Dodelson & Schmidt, 2020). Another thing to note is the usage of the convenient h throughout this paper. There are currently debates between astronomers as to the actual value of Hubble's Constant H_0 . Therefore, h is used

to scale H_0 to its value when the scientific community comes to a consensus about the value of H_0 . h is convenient because it is a dimensionless parameter, therefore it can be invoked to scale H_0 as needed.

1.2 The Λ CDM model

One of the most popular dark matter models within the dark matter framework is Λ Cold Dark Matter (CDM). As this model serves to be the basis of our paper, it would be sensible to first understand what the model encompasses. The "cold" refers to the fact that the model is non-relativistic¹ while the "dark" refers to the fact that it interacts with baryons and electromagnetic radiation at very low orders of magnitude. There are several CDM candidates that help explain the model, most notably WIMPs (Weakly Interacting Massive Particles), axions, and sterile neutrinos (Fairbairn, 2022). Λ is known as the cosmological constant and in essence represents dark energy. More specifically, it represents a form of energy density. Table 1 shows some of the parameters we will use to compute a matter-power spectrum (MPK) for the Λ CDM model. These values were taken from (Aghanim et al., 2020)

Table 1: Parameters for Λ CDM

$\Omega_B h^2$	0.0224 ± 0.0001
$\Omega_C h^2$	0.120 ± 0.001
h	0.67360
τ	0.054 ± 0.007
σ_8	0.811 ± 0.006

Most of these parameters remain constant and hence are omitted from future tables.

¹Moves at speeds far smaller than the speed of light

1.3 The Missing Sattelite Problem

Different dark matter models can explain the The Missing Satellite Problem (MSP), commonly known as the Dwarf Galaxy Problem, to different levels of accuracy. The MSP states that there is a discrepancy between the results of N-body simulations and actual observations regarding the distribution of dwarf galaxies near the Milky Way. Table 2, taken from (Klypin et al., 1999), outlines that there is indeed a discrepancy between observations and simulations.

Table 2: Dwarf Galaxy Discrepancy

Halo Mass ($h^{-1}M_{\odot}$)	Number of Satellites	Fraction of Mass in Satellites
2.93×10^{11}	9/15	0.053/0.112
3.90×10^{12}	39/94	0.041/0.049
1.22×10^{12}	27/44	0.025/0.051
6.26×10^{11}	5/10	0.105/0.135
2.74×10^{12}	24/52	0.017/0.029
5.12×10^{12}	37/105	0.055/0.112
1.33×10^{12}	24/58	0.048/0.049
7.91×10^{11}	17/26	0.053/0.067

While this discrepancy is significant by itself, it is exacerbated with the fact that observations and simulations match for normal-sized satellites. Therefore, this paper will be analysing various Matter power spectrums as well as their relative transfer functions with respect to Λ CDM for different dark matter models in order to find which model is best at explaining the MSP.

1.4 MPKs

Matter-Power spectrums are commonly referred to as MPKs because they are functions of the angular wave number k . They are usually represented as $P_x(k)$ where x can take on any dark matter model. They are two-point functions measured in Fourier Space (Dodelson & Schmidt, 2020). Another way to think of MPKs is as a distribution or autocorrelation function. MPKs are extremely

useful tools for analysis of the dwarf galaxy problem because they feed us density contrasts². Hence, regions with a high density contrast may be indicative of potential "missing" satellites. Using the Cosmic Linear Anisotropic Solving System (CLASS)(Blas et al., 2011), a coding environment in which cosmological simulations can be carried out, we are able to simulate a universe with different dark matter models. This enables us to plot an accurate MPK which will aid us in analysing the efficacy of the model in explaining the MSP. We can analytically solve for an MPK with the definition

$$P(k) = Ak^n T^2(k) \quad (6)$$

(Silva Neto, 2019)

where A is a normalisation constant and $T(k)$ is the transfer function (See section 1.5). However, to plot MPKs we will instead be using CLASS. This works by feeding in various parameters that illustrate a specific dark matter model such as the mass of a candidate and relative temperature. CLASS will then return data which can be used to plot an MPK. The upper error-tolerance limit on CLASS is approximately 4% (Blas et al., 2011), therefore we will not be including error bars given that it is a simulation. One thing to note is that the MPK we present is that of a primordial MPK³. As a result, the MPK acts as a remarkable peeping-hole into how dark matter in the early universe distributes itself after essentially splitting up into different chunks.

To start, we must first calculate the relative temperature of the dark matter candidate we are interested in exploring. This is given by:

$$T_{\text{relative}} = \frac{T_x}{T_\nu} = \sqrt[3]{\frac{10.75}{g_{dec}}} \quad (7)$$

²Differences between local densities and mean densities

³The MPK at the start of the universe

(Viel et al., 2005)

g_{dec} is the degrees of freedom at which decoupling, the process by which particles lose thermal equilibrium due to cosmic inflation (Viel et al., 2005), takes place. g_{dec} can be found by solving the equation given below from (Bode et al., 2001):

$$\Omega_x h^2 \approx \frac{115}{g_{dec}} \frac{g_x}{1.5 \text{ keV}} m_x \quad (8)$$

With plotted MPKs, we can form transfer functions that will aid us in our analysis.

1.5 Transfer functions

Transfer functions highlight small changes in a power spectrum dP for fluctuations in k , and thus will act as a helpful tool in our analysis. In context, a transfer function will enable us to identify the free-streaming scale of a particular dark matter model with respect to another dark matter model, as well as its breaking point, both of which will be explored later on in this paper. The transfer function, relative to a dark matter model, is defined as

$$T(k) = \sqrt{\frac{P_x(k)}{P_y(k)}} \quad (9)$$

where $P_x(k)$ and $P_y(k)$ are the MPKs of two different dark matter models. (Viel et al., 2005). It is often useful to characterise a fitting function for a specific transfer function. A common fitting function that works for Λ CDM and Λ Warm Dark Matter (Λ WDM) is given by:

$$T(k) = [1 + (\mu k)^{2\nu}]^{-\frac{5}{\nu}} \quad (10)$$

(Pordeus-da Silva et al., 2021) where

$$\mu = \alpha \left(\frac{g}{1.5} \right)^\kappa \left(\frac{m}{\text{keV}} \right)^{-1.1} (4\Omega_m)^{0.11} \left(\frac{10h}{7} \right)^{1.22} h^{-1} \text{Mpc} \quad (\text{Pordeus-da Silva et al., 2021})$$

$\Omega_m = \Omega_{dm} + \Omega_B$, and $\nu = 1.12$ for $k < 5 \, h\text{Mpc}^{-1}$. However, the fitting function does vary for different dark matter models.

2 Analysis of Dark Matter Models

2.1 ΛCDM

The model was explained in section 1.2. Therefore, this section will focus on the plotting of the MPK of ΛCDM . The following table (Table 3) shows an expanded version of Table 1, the uncertainty in $\Omega_x h^2$ was taken from (Aghanim et al., 2020).

<u>Table 3: Parameters for ΛCDM</u>	
$\Omega_x h^2$	0.120 ± 0.001
N_{cdm}	1
T_{relative}	0.71611 K

By passing this into CLASS, we are able to plot the MPK for ΛCDM as shown in figure 3.

The MPK by itself is not very helpful in analysing how well it explains the MSP. Therefore, we will now be plotting the MPKs and relative transfer functions with respect to ΛCDM for other dark matter candidates in order to contrast each model.

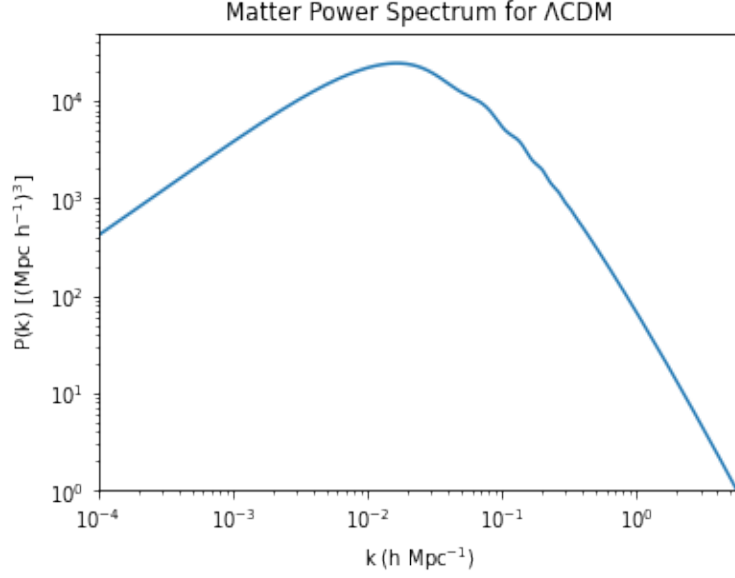


Figure 3: MPK of Λ CDM

2.2 WDM Neutrino

The next model we decided to settle on was a neutrino of mass 1 keV. Neutrinos are helpful models due to the fact that they act as thermal relics, which causes them to decouple before neutrinos at a free-streaming length of about 0.3 Mpc (Viel et al., 2005). By probing its g_x , which has a value of 1.5, we get the following parameters to plot its MPK:

Table 4: Parameters for Λ WDM

$\Omega_x h^2$	0.120
N	2
T_{relative}	0.19555 K

The MPK of the WDM Neutrino model is very similar to that of Λ CDM. Hence, for clarity, both of their MPKs were plotted on the same set of axes in order to spot the differences more clearly. The point at which the two MPKs

start to disagree with each other is known as the breaking point. This causes a downward shift of the MPK at small values of k (Large values of λ since $k = \frac{1}{\lambda}$). Figure 4 shows that the MPK for Λ WDM is shifted slightly below that of Λ CDM. This indicates that in a universe governed by Λ CDM, dark matter chunks are tightly packed at smaller scales. Hence, this dark matter forms galaxies while regular matter free streams as time goes on.

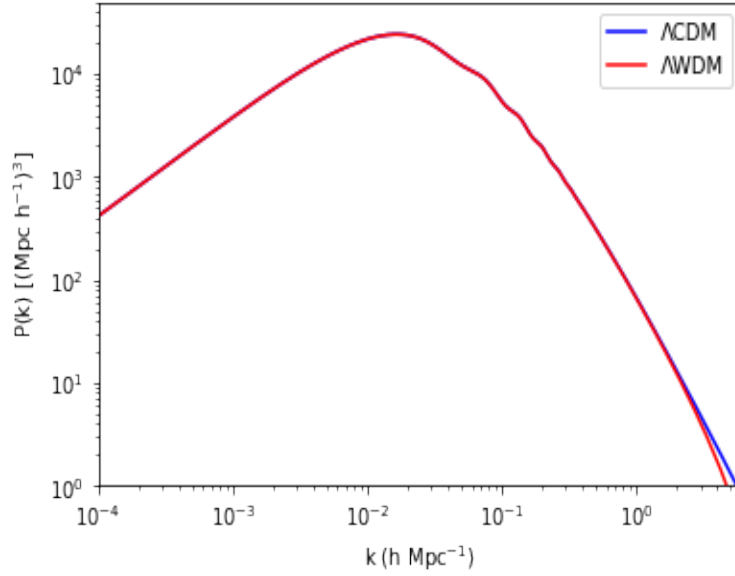


Figure 4: MPK of Λ CDM and Λ WDM

The slight wobbles at around $k = 10^{-1}$ is due to Baryonic Acoustic Oscillations⁴ (Silva Neto, 2019). These wobbles are better explained using the Cosmic Microwave Background Anisotropy Spectrum. However, this will not be explored in this paper. One can only analyse so much accurately with just the MPKs. Therefore, it may be more prudent to plot the relative transfer function, as shown by figure 5. The initial flat section is the section in which the two MPKs agree. This tells us that both models are fairly accurate to an

⁴Soundwaves produced at the beginning of the universe

extent given that the number of galaxies that can form for that value of k has already been constrained (Klypin et al., 1999). However, the relative transfer function tells us that Λ WDM is slightly more accurate given that the model agrees with the constrained section and at the same time predicts that there are fewer galaxies that should actually form (this is in accordance with N-body simulations)

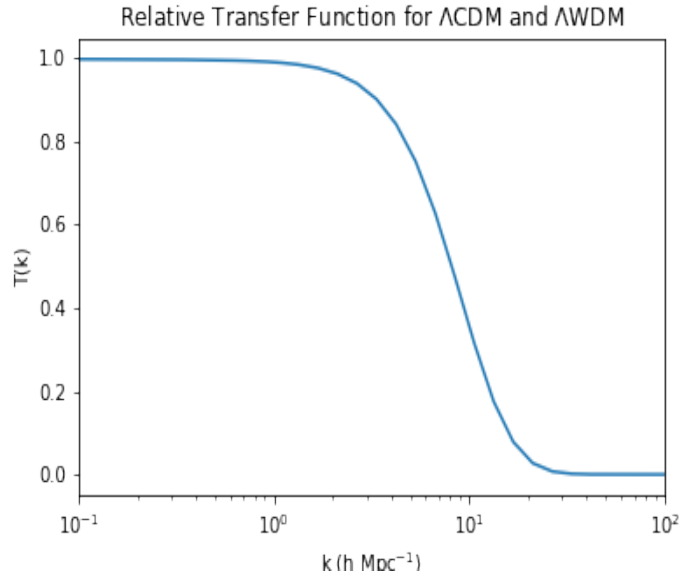


Figure 5: Relative Transfer function for Λ CDM and Λ WDM

It is also useful to find a fitting function for this transfer function (See section 2.3).

2.3 Changing g_x and fitting $T(k)$

In order to allow for some degree of exploration, but at the same time constrain complexity, we decided to simulate dark matter particles with different spin degrees of freedom. Thus, the only parameter that was changed between these particles and the WDM Neutrino counterpart was its g_x . We chose the values

of 3.0, 4.5, and 6.0 respectively. Table 5 below shows the different T_{relative} for each value of g_x that was used in CLASS. With this data, we were able to plot the following relative transfer functions for each model with respect to ΛCDM . This is shown in figure 6.

Table 5: g_x and its corresponding $T_{\text{relative}}(\text{K})$

3.0	0.15521
4.5	0.13559
6.0	0.12319

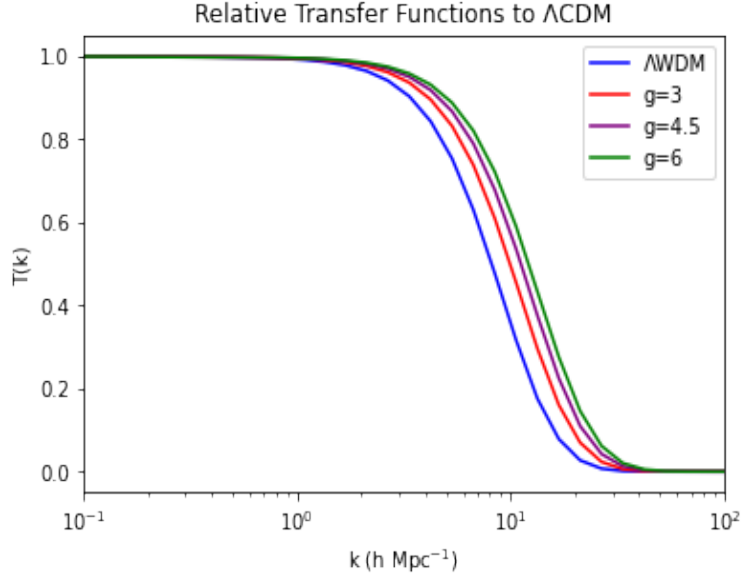


Figure 6: Relative Transfer functions

Before we analyse the transfer functions, it would be useful to consider their fitting functions. Equation 10 approximates a good fitting function for the following relative transfer functions. In order to find the values of α , κ , and ν , we used the scipy Python library. By considering a meshgrid function of k and the different values of g_x , we were able to create a transthermal fit function. We

used the following guesses for `scipy.optimize.curve_fit`.

Table 6: Guesses for fitting function

α	0.049
κ	-1.0
ν	1.12

These were informed guesses using values from literature such as (Viel et al., 2005). Running the transthermal fit function gave us the following values:

Table 7: Values for fit functions

α	0.0357968
κ	-0.28722415
ν	1.05880987

Substituting these values into equation 10 would yield us the fitting functions for the relative transfer functions.

In order to analyse the transfer functions, we must consider the fact that as the spin degree of freedom increases, the transfer function shifts to the right. In this case, g_x is analogous to mass as a similar result is expected if the mass of our dark matter model was to increase (mass was kept constant for sake of simplicity). These shifts show us that as g_x increases, the dark matter becomes colder as it ends up decoupling much later than Λ WDM. This causes its free streaming length to increase which causes less disruption to small scale structures, thereby causing a disparity with results from N-body simulations. Hence, Λ WDM slows down the growth of these structures and supresses $P(k)$ at scales smaller than the free-streaming length. This plot essentially enables us to fine-tune the missing satellite problem. One major part of the problem is that the scale of the disparity as well as the values of k at which the problem actually occur is unknown. Therefore, these plots help us show that warmer dark matter models are better at explaining the missing satellite problem in the first place.

Conclusion

Over the course of this paper we have shown that the Λ CDM model is not the best model at explaining the MSP. While, to an extent, reality matches the description of the model (as shown by the flat part of its MPK), it is not as accurate after a certain point. Thus, in order to help explain the model, we need to invoke warmer dark matter models. This paper has by no means "solved" the MSP, nor does it say that one dark matter model is far superior than the other. Instead, we have come to the conclusion that warmer dark matter models help explain the disparity between reality and N-body simulations as free-streaming length increases. As a result, small scale structures which have been observed to maintain stability are unchanged by the model. This paper shows the differences between the different dark matter models and how each model has its own benefits and limitations. It may be more prudent to study the MSP in greater depth with access to more technology as it may give way to a need for a "standard model for dark matter". In fact, the very dark matter that permeates our universe could be a soup of different dark matter models. Only more research will tell.

Acknowledgements

I would like to give my sincere gratitude to my supervisor and mentor Cannon Vogel. Without his constant support, this paper would not exist. I would also like to thank the Lumiere Research Scholars Program for the unforgettable experience.

References

- Aghanim, N., Akrami, Y., Ashdown, M., et al. 2020, *Astronomy & Astrophysics*, 641, A6
- Blas, D., Lesgourgues, J., & Tram, T. 2011, *Journal of Cosmology and Astroparticle Physics*, 2011, 034
- Bode, P., Ostriker, J. P., & Turok, N. 2001, *The Astrophysical Journal*, 556, 93
- Carignan, C., Chemin, L., Huchtmeier, W. K., & Lockman, F. J. 2006, *The Astrophysical Journal*, 641, L109
- Dodelson, S., & Schmidt, F. 2020, *Modern cosmology* (Academic Press)
- Fairbairn, M. 2022, *Symmetry*, 14, 812
- Klypin, A., Kravtsov, A. V., Valenzuela, O., & Prada, F. 1999, *The Astrophysical Journal*, 522, 82
- Pordeus-da Silva, G., Batista, R., & Medeiros, L. 2021, *Journal of Cosmology and Astroparticle Physics*, 2021, 062
- Silva Neto, J. P. d. 2019, B.S. thesis, Universidade Federal do Rio Grande do Norte
- Viel, M., Lesgourgues, J., Haehnelt, M. G., Matarrese, S., & Riotto, A. 2005, *Physical Review D*, 71, 063534
- Williams, D. R. 2010, Nasa,[Online]. Available: <https://nssdc.gsfc.nasa.gov/planetary/factsheet/>[Accessed 13 9 2021]